PHILOSOPHICAL TRANSACTIONS OF THE ROYAL SOCIETY B

Phil. Trans. R. Soc. B (2011) **366**, 3316–3329
doi:10.1098/rstb.2011.0045

Research

Variations in Amazon forest productivity correlated with foliar nutrients and modelled rates of photosynthetic carbon supply

Lina M. Mercado[1,2,*], Sandra Patiño[2,3], Tomas F. Domingues[4], Nikolaos M. Fyllas[5], Graham P. Weedon[6], Stephen Sitch[5,7], Carlos Alberto Quesada[5,12], Oliver L. Phillips[5], Luiz E. O. C. Aragão[7], Yadvinder Malhi[8], A. J. Dolman[9], Natalia Restrepo-Coupe[10,14], Scott R. Saleska[10], Timothy R. Baker[5], Samuel Almeida[11], Niro Higuchi[12] and Jon Lloyd[5,13]

[1]*Centre for Ecology and Hydrology, Wallingford, Oxon OX10 8BB, UK*
[2]*Max Planck Institute for Biogeochemistry, 07745 Jena, Germany*
[3]*Universidad Nacional de Colombia sede Amazonia, Km 2 via Tarapacá, Leticia, Amazonas, Colombia*
[4]*School of GeoSciences, University of Edinburgh, Drummond Street, Edinburgh EH8 9XP, UK*
[5]*School of Geography, University of Leeds, Leeds LS2 9JT, UK*
[6]*Met Office Hadley Centre, JCHMR, Wallingford, Oxon OX10 8BB, UK*
[7]*School of Geography, University of Exeter, Exeter EX4 4QF, UK*
[8]*Environmental Change Institute, School of Geography and the Environment, University of Oxford, Oxford OX1 3QY, UK*
[9]*VU University of Amsterdam, 1081 HV, Amsterdam, The Netherlands*
[10]*Ecology and Evolutionary Biology, University of Arizona, Tucson, AZ 85721, USA*
[11]*Museu Paraense Emílio Goeldi, Avendia Magalhães Barata 376, São Braz, Belém, Pará, Brasil*
[12]*Instituto Nacional de Pesquisas da Amazônia, Avenida André Araújo, 2936, Aleixo, CEP 69060-001, Manaus, AM, Brazil*
[13]*James Cook University, PO BOX 6811, Cairns, Queensland 4870, Australia*
[14]*Plant Functional Biology and Climate Change Cluster, University of Technology, Sydney, PO Box 123, Broadway NSW 2007, Australia*

The rate of above-ground woody biomass production, W_P, in some western Amazon forests exceeds those in the east by a factor of 2 or more. Underlying causes may include climate, soil nutrient limitations and species composition. In this modelling paper, we explore the implications of allowing key nutrients such as N and P to constrain the photosynthesis of Amazon forests, and also we examine the relationship between modelled rates of photosynthesis and the observed gradients in W_P. We use a model with current understanding of the underpinning biochemical processes as affected by nutrient availability to assess: (i) the degree to which observed spatial variations in foliar [N] and [P] across Amazonia affect stand-level photosynthesis; and (ii) how these variations in forest photosynthetic carbon acquisition relate to the observed geographical patterns of stem growth across the Amazon Basin. We find nutrient availability to exert a strong effect on photosynthetic carbon gain across the Basin and to be a likely important contributor to the observed gradient in W_P. Phosphorus emerges as more important than nitrogen in accounting for the observed variations in productivity. Implications of these findings are discussed in the context of future tropical forests under a changing climate.

Keywords: modelling photosynthesis; nutrient limitation; Amazon forest

1. INTRODUCTION

Recent research has found large-scale variations in stem growth rates (the rate of new wood production into both boles and branches, W_P) as well as tree turnover rates (mean rates of tree recruitment and mortality) across Amazonia. In general, the forests of

* Author for correspondence (L.Mercado@exeter.ac.uk).

One contribution of 16 to a Theme Issue 'The future of South East Asian rainforests in a changing landscape and climate'.

western Amazonia are more dynamic, with younger and faster growing trees which have lower wood density than those of the central and eastern Amazon [1–3]. The scale of the variability is substantial, with W_P varying by more than a factor 2 [1].

Different hypotheses have been proposed to explain this spatial variability in W_P [1]. First, owing to the proximity of the Andes, forest soils in western Amazonia tend to be richer in nutrients than their counterparts in central and eastern Amazon [4,5], and therefore greater soil fertilities might explain the higher W_P found in the west. Indeed, W_P has been found to be related to soil P and soil N concentrations and soil C : N ratios for 59 sites across the Amazon Basin, and also partly related to the amount of rainfall and its spatial distribution [6]. Trees with higher foliar nutrient contents are generally associated with these more fertile soils of the western part of the Basin [7], and one possibility is that the influence of soil fertility on W_P is exerted via effects of foliar [N] and/or foliar [P] on the canopy-level gross primary productivity (G_P).

A second possibility is that G_P actually varies very little across the Amazon Basin, but that different patterns of carbon allocation to respiration and/or other above- and below-ground organs could also explain the observed variations in stem growth [1]. However, faster growing trees on high-nutrient soils from western sites seem to allocate nearly the same proportion of productivity to above and below ground as their counterparts in the slower growing central and eastern Amazon forests [8]. This result does not, however, exclude the possibility that the slower growing eastern forests expend a greater proportion of their G_P on respiration than on growth [9].

In this study, we test the first hypothesis by quantifying the extent to which variations in simulated G_P across the Amazon Basin can explain observed variations in W_P. To investigate the likely variability in G_P, we undertake a basin-wide application of a tropical forest canopy gas-exchange model, which has already been calibrated and validated at various sites across the Amazon Basin [10].

Under the assumption of nitrogen (N) limitation, leaf photosynthesis is usually modelled based on the measured linearity between photosynthetic capacity and foliar N content. This reflects the large investment of foliar nitrogen in photosynthetic machinery [11]. Nevertheless, for tropical ecosystems, it has been suggested that phosphorous (P) rather than nitrogen (N) may constrain productivity in lowland tropical rain forests. A relative abundance of N in tropical rainforests has been suggested from foliar and soil δ^{15}N measurements [12–14] as well as by high rates of nitrogen oxide emissions and considerable losses of nitrogen through leaching processes in many tropical forest systems [9]. This is consistent with the suggestion first made by Vitousek [15] that most tropical forests may be phosphorus- rather than nitrogen-limited and consistent with the few available studies showing a close correlation between photosynthesis and foliar [P] for tropical forest species [16]. In a cross-biome analysis of the influence of P on the linear relationship between the light-saturated rate of photosynthesis (A_{max}) and foliar [N], it was found that the slope of such linear relationship increases with leaf [P] [17]. This suggests that in P-limited ecosystems, the relationship between A_{max} and foliar [N] is constrained by low [P] availability.

Most recently, Domingues *et al.* [18] implemented P limitation into the main photosynthetic parameters of the Farquhar & von Caemmerer [19] photosynthesis model. The parametrizations for maximum RuBisCO activity (V_{max}) and electron transport capacity ($\mathcal{J}_{max}$) used leaf-level nutrient and photosynthesis measurements, taken across a precipitation gradient incorporating different types of woody species in West Africa. Initial tests showed that the model (which allows for both V_{max} and $\mathcal{J}_{max}$ to be limited by either N or P) can also successfully predict leaf-level photosynthetic rates for tropical trees in the Cameroon, Bolivia and Australia [18].

Here, we use an ecosystem canopy-scale photosynthesis model, validated using flux tower data from five sites in the Brazilian Amazon [10], to simulate G_P for 38 sites across the Amazon Basin incorporating possible nitrogen and/or phosphorus limitations using the parametrizations developed by Domingues *et al.* [18] and *in situ* measurements. Specifically, we examine to what extent the simulated G_P with constraints of foliar [P] and/or [N] can explain the observed variability in stem growth rates.

2. METHODS

(a) *Data*

(i) *Sites*

We simulate G_P for 38 primary lowland rainforest sites located in Colombia, Venezuela, Ecuador, Peru and Brazil (figure 1). For all sites foliar nutrients, specific leaf area (S) and leaf area index (L) data had already been collected as part of the work of the RAINFOR Consortium. Site descriptions are given in table 1.

(ii) *Leaf nutrient data (nitrogen and phosphorous) and specific leaf area*

Nitrogen and phosphorus concentrations for upper canopy leaves used to derive canopy photosynthetic parameters (V_{max} and $\mathcal{J}_{max}$) are as in Fyllas *et al.* [7] with around 20 trees sampled per plot, with average values for each (usually) 1 ha plot calculated here with a species abundance weighting *viz*:

$$\hat{\Theta} = \frac{N_s \sum_{t=1}^{n_s} \Theta_{t,s}/n_s}{\sum_{s=1}^{m} N_s}, \tag{2.1}$$

where $\hat{\Theta}$ represents the plot-level estimate for the average value of any parameter, Θ, N_s is the number of times that any species, s, occurs in the plot, n_s is the number of times that species was actually sampled in the plot, m is the total number of species sampled in the plot and $\Theta_{t,s}$ represents individual measurement of parameter Θ on tree number t of species, s. Effectively, equation (2.1) gives a species abundance-weighted estimate for the plot-level average value of Θ, with the estimate of $\hat{\Theta}$ taking into account the fact that different species have different characteristic nutrient concentrations [7] as well as vastly varying relative abundances in different plots.

(iii) *Soil phosphorous*

Observed total soil phosphorus concentrations [21] available at 33 out of the 38 studied sites are taken from Quesada *et al.* [5].

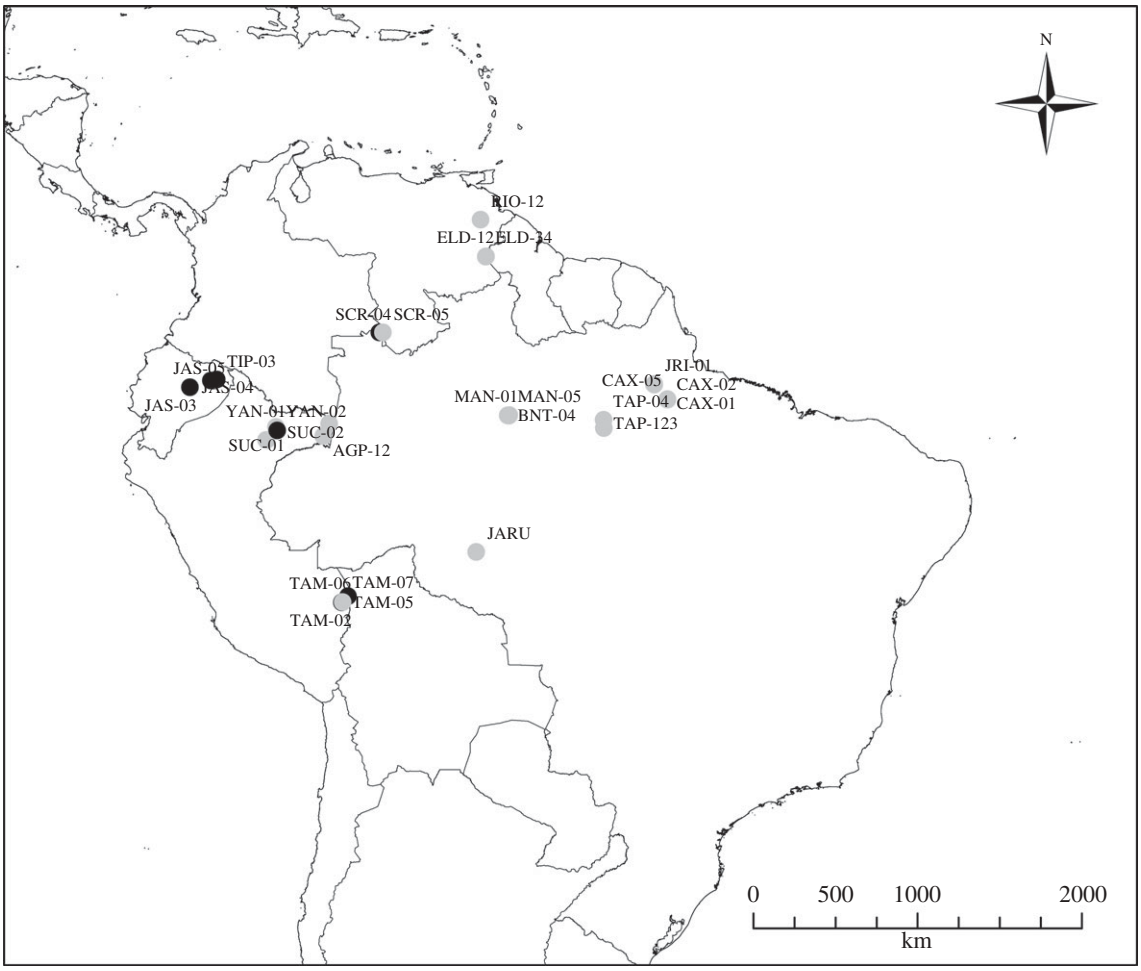

Figure 1. Rainforest site locations used in this study. Black and grey symbols denote N- and P-limited sites, respectively, according to Domingues *et al.* [18] parametrization (equation 2.2).

(iv) *Leaf area index*

Leaf area index (L) was derived from around 20 hemispherical photographs per site [22], these usually having been taken at the end of the rainy season (S. Patiño 2001–2004, unpublished data). For the JARU site, L was taken from the estimate of Meir *et al.* [23]. We assume a constant L for each site, throughout the simulations.

(v) *Atmospheric carbon dioxide concentration*

Six-monthly atmospheric [CO_2] from 1982 to 2001 (340 to 373 μmol mol^{-1}) were used as input data [24]. Although significant diurnal variations in [CO_2] may occur both above and within tropical forest canopies [25], neglecting this diurnal variability should not have a major impact on the overall estimate of G_P.

(vi) *Climatology*

The WATCH Forcing Data were used to provide sub-daily meteorology, and are based on the ERA-40 reanalysis regridded to half-degree with adjustment of meteorological variables for changes in elevation plus monthly adjustments based on observations [26,27]. The model input variables are solar radiation (downward shortwave radiation flux), wind speed, air temperature and specific humidity at three-hourly time steps, for the period 1980–2001. The monthly adjustments include for the downward shortwave radiation flux allowance for cloud fraction and the effects of both seasonal- and decadal-variations in atmospheric aerosol-loading, as well as the use of observed monthly average temperature and diurnal temperature range. The 38 sites are covered by 25 half-degree grid squares in the WATCH Forcing Data as some of the sites are adjacent to each other (figure 1).

(vii) *Data for validation*

Simulated values of mean annual gross primary productivity in the absence of foliar respiration (G_P^*, defined as G_P plus canopy foliar respiration, R_C [28]) are compared against bottom-up estimates based on individual measurements of the different components of the forest carbon-cycle at the five sites where data were available. The individual components included branch production, litterfall, tree growth, fine root production and autotrophic- and heterotrophic-respiration [8,29–31] (Y. Malhi, L. E. O. C. Aragão & D. B. Metcalfe 2005–2006, unpublished data). The methodology was standardized across all sites, in eastern Amazonia at Caxiuana (CAX-06) and western Amazonia at Tambopata, Peru (TAM-04 and TAM-05), but for sites located in central Amazon at Manaus (MAN-K34, denoted here MAN-01) and at Tapajos (TAP-04), G_P^* was derived from component measurements presented in the literature [31].

Eddy correlation estimates of G_P^* have been calculated by subtracting daytime measured net ecosystem exchange from ecosystem respiration (measured during

Table 1. Description of sites. Latitude (lat) and longitude (long) are given in decimal degrees, altitude (alt) in m, precipitation (precip) in mm and temperature (temp) in degrees Celsius. Soil types are taken from Quesada *et al.* [5] and remaining information is taken from Patiño *et al.* [20]. Sites in bold are nitrogen-limited according to equation (2.2).

plot	plot code	lat	long	alt.	precip	temp	soil type	forest type
AGP-12	Colombia	−3.74	−70.31	109	3216	25.8	Plinthosol	Terra firme
ALP-11	Peru	−3.95	−73.43	126	2763	26.34	Gleysol	Terra firme
ALP-12	Peru	−3.95	−73.44	133	2763	26.34	Alisol	Terra firme
ALP-21	Peru	−3.95	−73.44	142	2763	26.34	Arenosol	Terra firme
ALP-22	Peru	−3.95	−73.44	137	2763	26.34	Plinthosol	Terra firme
ALP-30	Peru	−3.95	−73.43	144	2763	26.34	Arenosol	Tall caatinga
BNT-04	Brazil	−2.63	−60.15	103	2272	27.08	Ferrasol	Terra firme
BOG-02	**Ecuador**	**−0.70**	**−76.48**	**271**	**3252**	**25.67**	**Cambisol**	**Terra firme**
CAX-01	Brazil	−1.74	−51.46	15	2314	26.88	Acrisol	Terra firme
CAX-02	Brazil	−1.74	−51.46	15	2314	26.88	Acrisol	Terra firme
CAX-06	Brazil	−1.72	−51.46	15	2314	26.88	Ferrasol	Terra firme
CUZ-03	**Peru**	**−12.50**	**−68.96**	**190**	**2417**	**25.54**	**Cambisol**	**Terra firme**
ELD-12	Venezuela	6.10	−61.40	201	1977	26.66	Cambisol	Terra firme
ELD-34	Venezuela	6.08	−61.41	369	1977	25.82	Leptosol	Terra firme
JARU	Brazil	−10.08	−61.93	150	1600	26	Acrisol	Terra firme
JAS-02	Ecuador	−1.07	−77.62	434	4013	23.38	Alisol	Terra firme
JAS-03	Ecuador	−1.08	−77.61	410	4013	23.38	Alisol	Terra firme
JAS-04	Ecuador	−1.07	−77.61	430	4013	23.38	Alisol	Terra firme
JAS-05	**Ecuador**	**−1.06**	**−77.62**	**394**	**4013**	**23.38**	**Fluvisol**	**Terra firme**
JRI-01	Brazil	−0.89	−52.19	127	2346	26.59	Ferrasol	Terra firme
LOR-12	Colombia	−3.06	−69.99	94	3216	25.8	Plinthosol	Terra firme
MAN-01	Brazil	−2.61	−60.21	100	2950	26.7	Ferrasol	Terra firme
MAN-05	Brazil	−2.61	−60.20	100	2950	26.7	Ferrasol	Terra firme
RIO-12	Venezuela	8.11	−61.69	270	1239	25.62	Lixisol	Terra firme
SCR-05	Venezuela	1.93	−67.04	111	3093	25.98	Acrisol	Tall caatinga
SCR-04	**Venezuela**	**1.93**	**−67.04**	**110**	**3093**	**25.98**	**Podzol**	**Terra firme**
SUC-01	Peru	−3.25	−72.91	123	2671	26.29	Plinthosol	Terra firme
SUC-02	Peru	−3.25	−72.90	122	2671	26.29	Acrisol	Terra firme
TAM-01	Peru	−12.84	−69.29	205	2417	25.2	Alisol	Terra firme
TAM-02	Peru	−12.83	−69.29	210	2417	25.2	Alisol	Terra firme
TAM-05	Peru	−12.83	−69.27	220	2417	25.2	Cambisol	Terra firme
TAM-06	**Peru**	**−12.84**	**−69.30**	**200**	**2417**	**25.2**	**Alisol**	**Terra firme**
TAM-07	Peru	−12.83	−69.26	225	2417	25.2	Cambisol	Terra firme
TAP-123	Brazil	−3.31	−54.94	187	1968	26.13	Ferrasol	Terra firme
TIP-03	**Ecuador**	**−0.64**	**−76.14**	**237**	**3252**	**25.79**	**Gleysol**	**Terra firme**
YAN-01	Peru	−3.44	−72.85	104	2671	26.31	Alisol	Terra firme
YAN-02	**Peru**	**−3.43**	**−72.84**	**104**	**2671**	**26.31**	**Cambisol**	**Terra firme**

night). The method to derive ecosystem respiration from night-time measurements is explained elsewhere [32–34]. Hourly night-time net ecosystem exchange measurements include a correction during periods of low turbulence using a friction velocity threshold [35]. A measure of the night-time friction velocity uncertainty of fluxes is presented using the upper and lower bounds of the friction-velocity threshold used for corrections as in Saleska *et al.* [34].

Mean annual values of G_P^* from eddy correlation at MAN-01, TAP-04 and an additional tower at Jaru (southwestern Amazon) were calculated from monthly mean values [36] taking the mean of all available years with an uncertainty bound explained above. Mean annual G_P^* at MAN-05 and CAX-06 are taken from table 12 in Malhi *et al.* [31].

(viii) *Stem wood production* (W_P) *and basal area growth* ΔB *data*

Recent estimates for W_P and basal area growth ΔB were available for 35 sites taken from Quesada *et al.* [4], and supplemented in a few cases with unpublished data from the RAINFOR database [37]. The methodology for these measurements is described in detail elsewhere [1,38] and is based on tree-by-tree records of long-term diameter growth over multiple intervals that total on average greater than 10 years per plot, and applies mean measured species-level wood densities, stand-level allometric models and census-interval corrections to estimate stand-level wood production.

(b) *Model, modelling approach and parametrization*

The canopy-scale photosynthesis model [10,39] uses the C_3 leaf photosynthesis model from Farquhar & von Caemmerer [19] and the sun and shade approach from de Pury & Farquhar [40] to scale from leaf- to canopy-level, and assumes an optimization of stomatal behaviour [41]. The model has been calibrated and evaluated at five eddy covariance sites in the Brazilian Amazon.

Photosynthetic parameters (V_{cmax} and $\mathcal{J}_{max}$) were parametrized using two approaches. First, using

eqn (2) from Domingues *et al.* [18] which includes both N and P constraints on photosynthesis and a leaf structure term S, specific leaf area, in ($cm^2\ g^{-1}$). These 'min{N : P}' relationships are:

$$V_{max}^{DW} = \min\{a_{NV}[N]_{DW} + b_{NV}S + c_{NV};\ a_{PV}[P]_{DW} + b_{PV}S + c_{PV}\}$$

and

$$\mathcal{J}_{max}^{DW} = \min\{a_{NJ}[N]_{DW} + b_{NJ}S + c_{NJ};\ a_{PJ}[P]_{DW} + b_{PJ}S + c_{PJ}\}, \quad (2.2)$$

where V_{max}^{DW} and $\mathcal{J}_{max}^{DW}$ are V_{max} and $\mathcal{J}_{max}$ expressed on a leaf dry-weight basis ($\mu mol\ g^{-1}\ s^{-1}$), subsequently converted to area basis using the specific leaf area S, with $[N]_{DW}$, $[P]_{DW}$ expressed in $mg\ g^{-1}$ DW. The empirical coefficients from equations (2.2) are

$$a_{NV} = 0.43, b_{NV} = 0.368, c_{NV} = -1.559,$$
$$a_{PV} = 0.453, b_{PV} = 0.25, c_{PV} = -0.798$$

and

$$a_{NJ} = -0.406, b_{NJ} = 0.447, c_{NJ} = -1.496,$$
$$a_{PJ} = 0.436, b_{PJ} = 0.318, c_{PJ} = -0.741$$

with a coefficients in ($\mu mol\ mg^{-1}\ s^{-1}$), b coefficients in ($\mu mol\ cm^{-2}\ s^{-1}$) and c coefficients in ($\mu mol\ g^{-1}\ s^{-1}$).

The remaining parameter values, from the photosynthesis model, are assumed invariant across all sites and are as follows: temperature sensitivities of V_{max} and $\mathcal{J}_{max}$, S_J ($693.124\ J\ mol^{-1}\ K^{-1}$) and H_J ($220\,000\ J\ mol^{-1}$), respectively; the curvature factor (0.7 unit less) of the potential rate of electron transport equation, quantum yield of photosynthesis (0.35 mol electrons mol^{-1} photons) and λ for the stomatal conductance model being 1200 mol mol^{-1}.

(i) *Scaling up from leaf- to canopy-level*

Canopy-level values of V_{max}, $\mathcal{J}_{max}$ and leaf respiration R_d were estimated as the integral of the vertical profile of their leaf-level values over the entire canopy leaf area (L) following the method of de Pury & Farquhar [40], as implemented and applied in Mercado *et al.* [39] and Mercado *et al.* [10]. Canopy-level maximum carboxylation activity of RuBisCO $\hat{V}_{max}^{C}$ ($\mu mol\ m^{-2}\ s^{-1}$), is estimated as

$$\hat{V}_{max}^{C} = \frac{\hat{V}_{max}[1 - e^{-k_P L}]}{k_P}, \quad (2.3)$$

where $\hat{V}_{max}$ is the estimated RuBisCO activity at the top of the canopy obtained by the relevant substitutions of and $[\hat{N}]$, $[\hat{P}]$ and/or $\hat{S}$ into equation (2.2) and k_P is the extinction coefficient for photosynthetic capacity that defines how photosynthetic capacity decreases with the cumulative L downwards from the top of the canopy. Low values of k_P mean shallow profiles of photosynthetic capacity, and thus for any given values for $\hat{V}_{max}$ and L then $\hat{V}_{max}^{C}$ increases with decreasing k_P.

The upper canopy photosynthetic capacity parameter estimates, $\hat{V}_{max}$ and $\hat{\mathcal{J}}_{max}$, were estimated using equation (2.2) with R_d being estimated as a constant fraction of $\hat{V}_{max}$ (0.022) [10]. We calculate the extinction coefficient k_P using the equation derived by Lloyd *et al.* ([28], fig. 10) from a compilation of data from different sources from broadleaf forest and trees, *viz*:

$$\log(k_p) = 0.00963\hat{V}_{max} - 2.43, \quad (2.4)$$

where $\hat{V}_{max}$ is in the units of $\mu mol\ m^{-2}\ s^{-1}$.

From equation (2.4), 'k_P' increases with increasing $\hat{V}_{max}$. This means that plants with high upper-leaf photosynthetic capacities have relatively steeper vertical canopy photosynthetic profiles than plants with low values of upper-leaf photosynthetic capacities which have shallower profiles.

We incorporate an inhibition of leaf respiration with light [42] where for any leaf in the canopy, R_d is reduced by 30 per cent when its incident irradiance, I, is higher than 10 $\mu mol\ m^{-2}\ s^{-1}$.

(ii) *Outline of simulations and analysis*

- Canopy photosynthesis is simulated using the parametrizations given by the 'min{N : P}' equations and model evaluation is assessed with available observations from single components of the ecosystem carbon balance (the so-called 'bottom up') and also from eddy correlation.
- Additionally, the following sensitivity tests are performed. (i) A control simulation at which $\hat{V}_{max}$ and $\hat{\mathcal{J}}_{max}$ are held constant (to the mean value for all sites given by the 'min{N : P}' equations), in order to assess the climate effect on simulated G_P when compared with simulations with variable parameters, (ii) a set of simulations assuming N limitation, and (iii) P limitation at all sites using the 'min{N : P}' equations.
- Relationships between simulated G_P (under all model configurations), observed leaf nutrients (N,P), total soil P and observed stem wood production (W_P) and basal area growth (ΔB) are provided (at 33 sites where all data are available) and linear-adjusted Pearson correlation coefficient (R^2) is used to assess how the above given variables are related.

3. RESULTS

(a) *Leaf nutrients*

As shown in figure 2, $[\hat{P}]$ varies by a factor of 3–4 when expressed on either an area or dry-weight basis and with $[\hat{N}]$ varying less across the 38 sites. The highest $[\hat{P}]$ content was found at some of the western sites in Ecuador and Peru while the lowest values are found in eastern Brazil. Lowest $[\hat{N}]$ values were at some of the sites in northeast Venezuela and were highest in Ecuador, north and south Peru. As $[\hat{P}]$ increases, $[\hat{N}] : [\hat{P}]$ ratios decrease from *ca* 40 to 10.

(b) *Relationship between foliar (N,P) and soil (P) nutrients to observed stem wood production (W_P) and basal area growth (ΔB)*

Figure 3 illustrates relationships between measured $[\hat{N}]$ and $[\hat{P}]$ in leaves on a dry-weight and area basis with W_P (top row) and ΔB (bottom row). Additionally, the figure shows the relationships between measured total soil P with W_P (top row) and ΔB (bottom row). Pearson's adjusted R^2 shows significant correlation ($p < 0.05$) between foliar P, on both dry-weight and

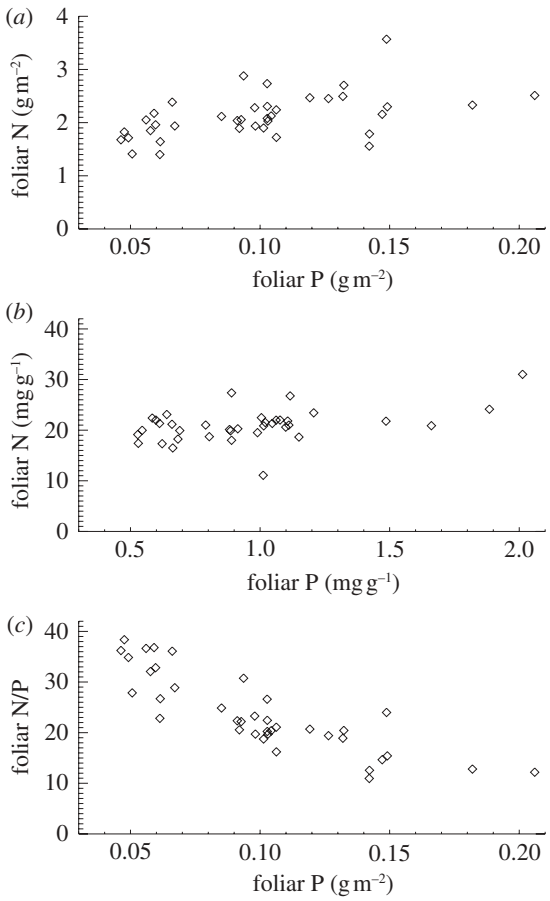

Figure 2. Variability of foliar [$\hat{N}$] and [$\hat{P}$] on (*a*) area basis, (*b*) dry-weight basis and (*c*) their N : P ratio. Data taken from Fyllas *et al.* [7].

area basis with W_P and ΔB. Total soil P is also significantly correlated with ΔB, but apparently not with W_P ($p = 0.062$). Foliar N is not correlated with W_P, but is correlated with ΔB, but only when expressed on an area basis. This suggests that P is more important than N at explaining some of the observed variability in stem-wood production and basal area growth. However, foliar P and foliar N are correlated with each other ($R = 0.54$, $p < 0.001$). Using partial correlation, foliar P is significantly correlated with W_P ($R = +0.49$, $p = 0.004$) controlling for foliar N. On the other hand, partial correlation of foliar N with W_P is not significant ($R = -0.06$, $p = 0.737$) after controlling for its correlation with foliar P. Using a canopy photosynthesis model, we now explore the extent to which P limitation to photosynthesis is more important than N limitation as implied by figure 3.

(c) *Relationship between simulated net carbon uptake and observed stem wood production (W_P) and basal area growth (ΔB)*

Simulated mean annual G_P^*, averaged over the period 1980–2001 for all sites, as shown in table 2, ranges from 30.9 Mg C ha^{-1} a^{-1} for CAX-01 in eastern Amazonia to 41.2 Mg C ha^{-1} a^{-1} for JAS-05 in Ecuador.

In figure 4, the relationships between simulated G_P and observed W_P (top row) and ΔB (bottom row) are illustrated for four model configurations with various combinations of $\hat{V}_{max}$ and $\hat{\mathcal{J}}_{max}$. For the first simulation, $\hat{V}_{max}$ and $\hat{\mathcal{J}}_{max}$ are taken as invariant across all sites using the mean dataset values obtained from equation (2.2). This simulation thus shows the effect of climate alone on simulated G_P. The remaining three simulations allow for between-site climate variability, but with different assumptions regarding the nature of nutrient limitations on tropical forest tree photosynthesis *viz*: (i) N limitation, (ii) P limitation, and (iii) both N and P limitation with $\hat{V}_{max}$ and $\hat{\mathcal{J}}_{max}$ calculated using the 'min{N : P}' relationship of equation (2.2) (figure 4).

Simulated G_P with invariant photosynthetic parameters showed no significant correlation with either W_P or ΔB. There was, however, a significant correlation between G_P simulated under N-limitation, under P-limitation, and under both N- and P-limitation with both W_P and ΔB. From the relationships with W_P, simulated G_P under P-limitation (adjusted $R^2 = 27.4\%$) explains nearly the same observed variability as when both N and P are limiting (adjusted $R^2 = 26.25\%$). From the relationships with ΔB, simulated G_P under P-limitation (adjusted $R^2 = 48.2\%$) explains less observed variability than when both N and P are limiting (adjusted $R^2 = 60.5\%$). This means that, when explaining basal area growth, N becomes important as well. This is consistent with figure 3, based on observations; it is clear that P is more important than N in accounting for variations in canopy photosynthesis that are relatable to the observed variability in stem wood production. However, in some circumstances to explain the basal area growth rates, a relatively low N availability is important.

(d) *Model evaluation*

Comparison of observed and modelled G_P^*, G_P and R_C at the few available sites (table 3 and figure 5) shows that simulated values are close to the observations, with simulated R_C closer to the bottom-up estimates (−5%). Comparison between G_P^* derived from bottom-up and eddy correlation shows much more variability in the bottom-up values. Simulated G_P^* using the 'min{N : P}' relationships is on average 14 and 7 per cent higher than the mean from bottom-up and eddy covariance estimates, respectively.

4. DISCUSSION

(a) *Model parametrization and implications for simulated G_P*

Although the parametrization of Domingues *et al.* [18] was developed using a dataset based on savannah and forest trees from West Africa, it performed surprisingly well, in as much that the predicted G_P correlated well with the observed values of W_P and ΔB across the Amazon Basin. Although it might be argued that this was more-or-less inevitable given the already strong correlation between foliar P and these growth parameters (figure 3), what is important here is that this result was obtained through the model results showing that most sites should be represented as phosphorus- rather than nitrogen-limited in order to account for the maximum range in woody growth rates (figure 4). Only a few sites were predicted to be nitrogen-limited (black in figure 1, filled circles in figures 3 and 4). These were located on either alisols, fluvisols or

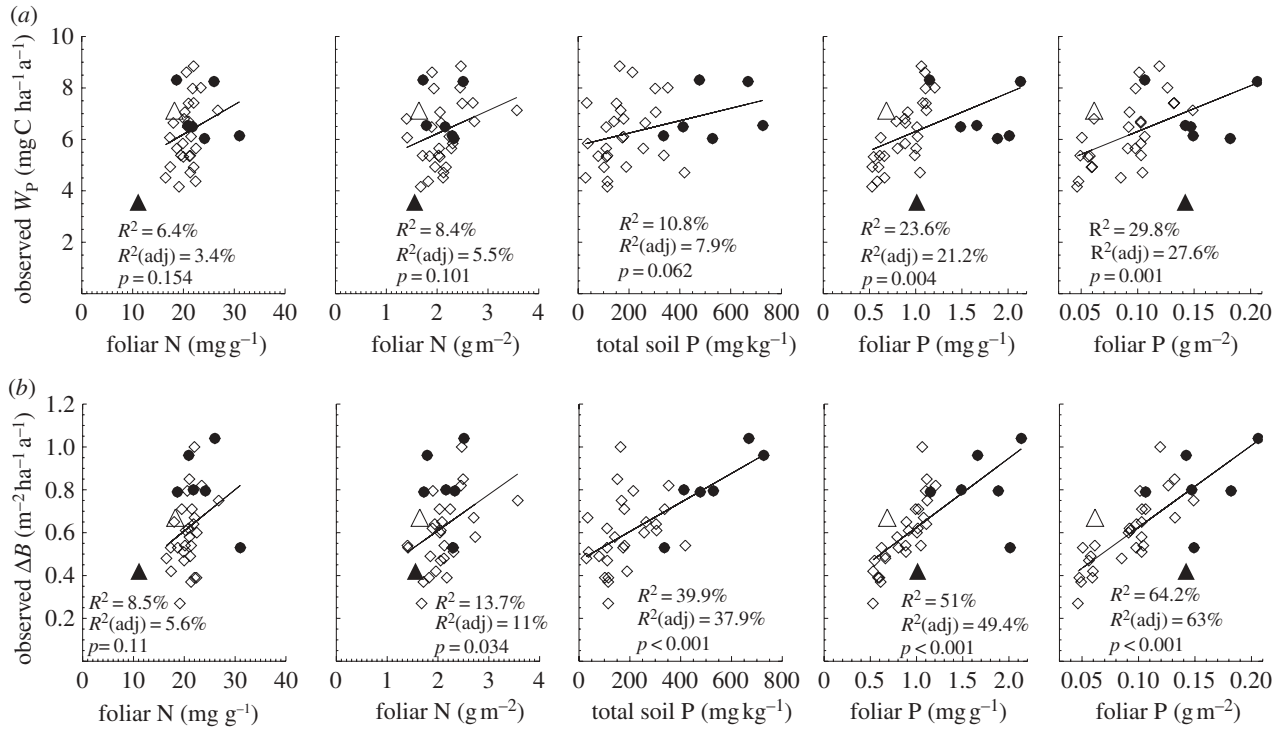

Figure 3. Relationships of foliar N and P (on dry-weight and area basis) [7] and soil P content [5] against (*a*) observed stem growth (W_P), (*b*) basal area growth (ΔB) [6] at 33 sites. Filled and open symbols correspond to N- and P-limited sites, respectively, according to equation (2.2). The triangle symbols correspond to sites with no available soil phosphorous data.

cambisols—all of which are relatively high in available soil phosphorus [5] or, in one case, on a podzol, this being a soil type for which nitrogen availability may be unusually low [5,12]. Nevertheless, despite some suggestion of N limitations (at seven sites), there was little practical difference between the 'P-limited' sites and 'min{N : P}' cases (figure 4, third and fourth columns) in their ability to predict either of the growth metrics investigated. This is because even when N-limitation was predicted, the modelled photosynthetic parameters under P-limitation were only marginally greater. For example at TIP-03, BOG-02 and YAN-02, it appears that N and P are co-limiting and $\hat{V}_{max}$ derived from $[\hat{N}]_A$ and $[\hat{P}]_A$ were 54.5 and 55.2 μmol m^{-2} s^{-1} at TIP03, 56.2 and 59.8 μmol m^{-2} s^{-1} at BOG-02 and 50.3 and 50.6 μmol m^{-2} s^{-1} at YAN-02, respectively. At the remaining four sites, more N-limitation was obtained (only three included in R^2 calculations), corresponding values for $\hat{V}_{max}$ derived from $[\hat{N}]_A$ and $[\hat{P}]_A$ were 59.7 and 69.1 μmol m^{-2} s^{-1} at JAS-05, 57.8 and 65.3 μmol m^{-2} s^{-1} at TAM-06, 50.3 and 56.4 μmol m^{-2} s^{-1} at CUZ-03 and 52.4 and 65.3 μmol m^{-2} s^{-1} at SCR-04. Finally, application of the Domingues *et al.* [18] parametrization to our dataset showed P-limitation at sites with foliar N : P ratios higher than 17. This is also the threshold value suggested for P-limitation in plants [43,44].

Indeed, it may be that because the small number of N-limited sites are used in the simple (but independent) parametrization of photosynthesis based on foliar [P] in area basis, the '$[P]_A$ only' equation of Mercado *et al.* [10] (equation A 1) gives as good relationship between G_P and both W_P and ΔB (figure 6) as the more complex 'min{N : P}' model of Domingues *et al.* [18]. Additionally, the related model predictions of G_P based on foliar [N] on area basis '$[N]_A$ only' (equation A 1) performs particularly poorly (figure 6). Indeed, the simple '$[P]_A$ only' equation actually gives rise to slightly higher R^2 than the 'min{N : P}' model. The reasons for this are unclear, but might have to do with the fact that the '$[P]_A$ only' relationship was empirically derived by fitting the canopy-scale model used in this study to eddy correlation data from just five sites, all located in poor-nutrient soils. Additionally, even though V_{max} parametrizations (equations (2.2) and A 1) were quantitatively similar at many sites (not shown), simulated G_P was higher with the '$[P]_A$ only relationship' (table 2). This is mostly because the ratio $\mathcal{J}_{max}/V_{max}$ was higher in those simulations (1.92 versus $\mathcal{J}_{max}/V_{max}$ ranging between 1.5 and 1.6), which translates into higher light-limited velocity of photosynthesis, and therefore simulated G_P under both sets of parametrizations is not strictly comparable.

The 'min{N : P}' parametrization was evaluated against single leaf V_{cmax} and $\mathcal{J}_{max}$ derived from gas exchange measurements at a site in Tapajos [18]. Results show no statistically significant difference between the mean predicted and observed values (mean values of predicted and observed V_{cmax} were 0.45 ± 0.09 and 0.39 ± 0.16 μmol g^{-2} s^{-1} and mean values of predicted and observed $\mathcal{J}_{max}$ were 0.69 ± 0.15 and 0.60 ± 0.22 μmol g^{-2} s^{-1}). Furthermore, estimates of V_{cmax} derived from gas exchange measurements for tropical rainforest in the Amazon are scarce. Here, we use the only five available data sources that we are aware of to compare against the top of the canopy V_{cmax} estimated in this study. Our estimates are close to, and within the range of, mean values inferred from gas exchange measurements at MAN-05 [45], CAX-06 [46] TAP-04 in Brazil [47] and LFB-02 in Bolivia (T. Domingues

Table 2. Simulated mean annual G_P^* in Mg C ha^{-1} a^{-1} for the period 1980–2001 using 'min {N : P}' (equation 2.2) and 'P_A-only' (equation A 1) model parametrizations.

site	'min{N : P}'	'P_A-only'
AGP-12	36.6	41.6
ALP-11	37.1	41.1
ALP-12	38.8	42.4
ALP-21	39.6	43.7
ALP-22	34.9	40.4
ALP-30	36.8	41.1
BNT-04	33.7	38.7
BOG-02	39.0	43.7
CAX-01	30.9	36.6
CAX-02	31.0	36.7
CAX-06	30.3	35.8
CUZ-03	37.6	44.4
ELD-12	32.3	38.6
ELD-34	35.1	40.5
JARU	35.2	39.8
JAS-02	40.8	44.8
JAS-03	38.8	43.1
JAS-04	38.0	42.5
JAS-05	41.2	46.7
JRI-01	34.6	38.6
LOR-12	37.1	41.8
MAN-01	34.3	39.4
MAN-05	35.8	40.6
RIO-12	33.3	40.5
SCR-04	36.2	43.0
SCR-05	36.2	39.4
SUC-01	37.2	41.8
SUC-02	37.5	41.7
TAM-01	36.2	40.7
TAM-02	35.8	40.5
TAM-05	33.4	38.6
TAM-06	40.8	46.0
TAM-07	34.7	39.3
TAP-04	35.7	40.4
TAP-123	33.3	38.6
TIP-03	37.1	43.2
YAN-01	38.5	43.2
YAN-02	37.0	42.1

2007, unpublished data), as shown in figure 7. Estimated $\mathcal{J}_{max}/V_{max}$ in this study ranged between 1.5 and 1.6 using the 'min{N : P}' relationship, which agrees well with published values for other tropical rainforest in the Amazon and in Africa. $\mathcal{J}_{max}/V_{max}$ values for upper-canopy leaves at Manaus [45], Caxiuana [46], Tapajos [47] and LSL-02 (T. Domingues 2007, unpublished data) have been reported as 2.27, 1.94, 1.59 and 1.92, respectively. Also, Coste *et al.* [48] reported a $\mathcal{J}_{max}/V_{max}$ ratio of 2.1 from seedlings of 14 tree species in the tropical forest of French Guiana. Meir *et al.* [49] obtained $\mathcal{J}_{max}/V_{max}$ ratios of 1.7 from gas exchange measurements at a rainforest in Cameroon with broadleaf, coniferous, shrubs and herbaceous plants.

(b) *Model evaluation*

The model evaluation presented in this study comparing simulated G_P^* against bottom-up and eddy covariance flux estimates is intended as a point of reference for the model only (i.e. as a general evaluation). This is because simulations correspond to an average over the period 1980–2001 and the available G_P^* estimates from both type of observations used in this study correspond to a different and shorter period of time, generally a few years at most.

There are errors associated with both methods used to estimate G_P^*, with both likely to underestimate the fluxes. Underestimation of total net ecosystem exchange using bottom-up approaches for tropical forest can potentially be up to 20 per cent [50]. There are also difficulties in estimating G_P^* from eddy covariance fluxes. Important sources of error from eddy covariance measurements include data representativity, treatment of data gaps, flux correction for systematic errors and the non-measured night-time fluxes [51]. The latter are associated with a frequent failure of the system to measure night-time fluxes during low wind speed conditions [34,52–54]. Therefore, only observations above a defined wind-speed threshold can be used for the purpose of estimating ecosystem respiration, R_e which is used together with the daytime net ecosystem exchange measurements to estimate G_P^* from eddy covariance. Unmeasured night-time fluxes can introduce significant errors into estimates of R_e [51]. Additionally, the response of R_e to daytime temperatures and a response of leaf respiration to both temperature and light conditions [42] are still unaccounted for in the calculation of R_e in the studied sites. However, although these effects might counteract each other, there are no available measurements to quantify them. As for daytime measurements, the total uncertainty estimated for the Manaus K34 and Jaru site are $\pm$12 and $\pm$32 per cent, respectively [55].

Once the difficulties in estimating G_P^* from bottom-up and eddy covariance measurements are considered, we conclude that our model estimates are in reasonable agreement. Furthermore, the canopy exchange photosynthesis model used in this study showed agreement of between $\pm$10 per cent with eddy covariance estimates of G_P^* at the five main eddy covariance sites (MAN-C14, MAN-K34, TAP-K67, Jarú and CAX-06, [10]), despite the photosynthesis/nutrient parametrizations. Similarly, our estimates of G_P^* agree with values reported for tropical humid evergreens in the global dataset of Luyssaert *et al.* [56] with estimates from the bottom-up approach (36 Mg C ha^{-1} a^{-1}, from six sites). Nevertheless, the main purpose of this study was to simulate variation in G_P across the Amazon Basin and to look for relationships with observed stem wood production (W_P) and basal area growth (ΔB) rather than to simulate the absolute value of G_P at any single site.

Evaluation of simulated leaf respiration (figure 5 and table 3) shows good model agreement against observations. Analyses with global datasets have shown a consistent coupling between mass-based respiration rates and $[N]_{DW}$ content across species [57]. In this study, we estimate leaf respiration rates at 25°C from V_{cmax}, but V_{cmax} is usually constrained by leaf P, according to our models. Although numerically our leaf respiration rates seem to match the scaled-up observations, it remains to be determined if this assumption is valid. Nevertheless, it is worth pointing out that Meir *et al.* [58] found high correlation between measured leaf respiration rates and foliar $[P]_A$, especially when specific leaf area was included in their analysis for the Jaru tower site.

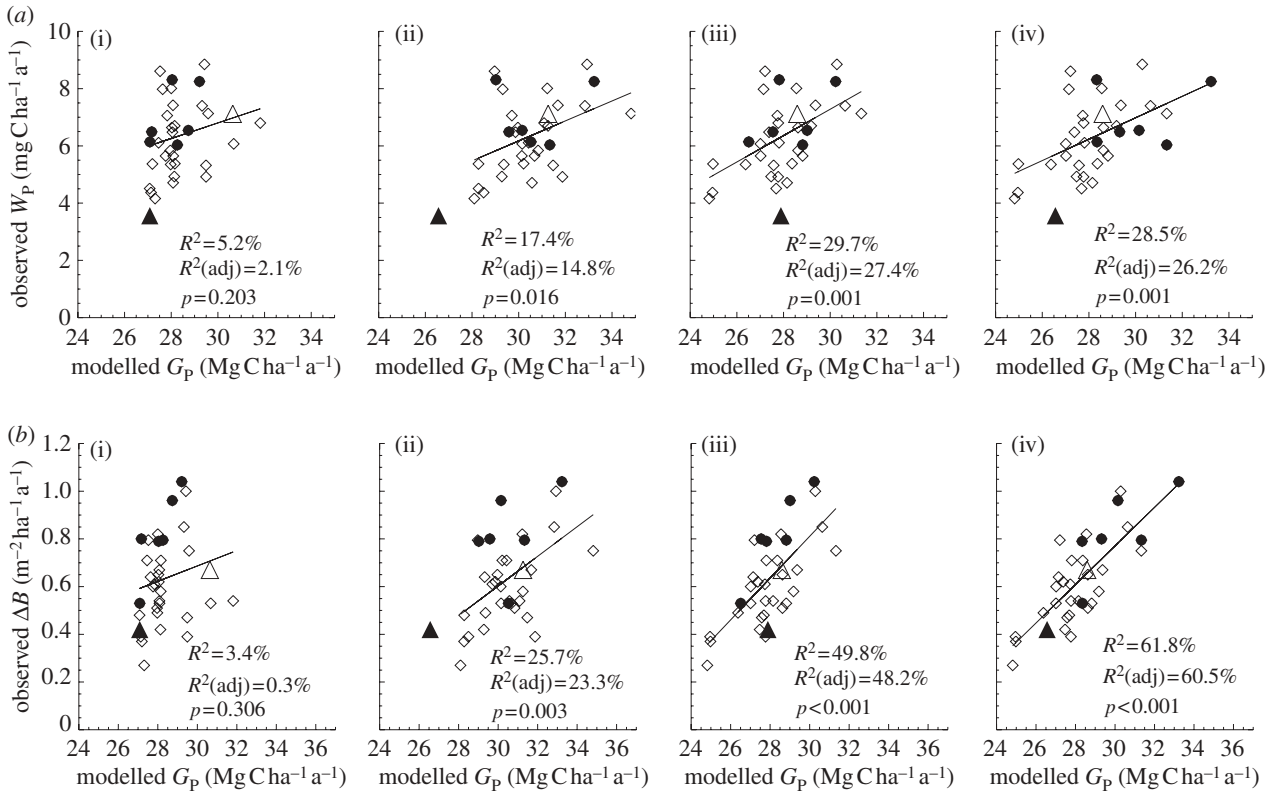

Figure 4. Relationships of simulated G_P (using the 'min{N : P}' relationship under four model configurations) against (*a*) observed stem growth (W_P), and (*b*) basal area growth (ΔB) [6] at 33 sites. Each of the four model configurations correspond to a column: (i) with invariant $\hat{V}_{max}$ and $\hat{\mathcal{J}}_{max}$, assuming (ii) N limitation, (iii) P limitation and (iv) both N and P limitation across all studied sites. Filled and open symbols correspond to N and P limited sites, respectively, according to equation (2.2). The triangle symbols correspond to sites with no available soil phosphorous data.

Table 3. Model evaluation of simulated gross primary productivity in the absence of foliar respiration (G_P^* defined as G_P plus canopy foliar respiration, R_C), G_P and R_C in Mg C ha^{-1} a^{-1} using available observations from 'bottom-up' and eddy correlation. Upper and lower bounds of uncertainty correction for eddy correlation values are related to a night-time friction velocity threshold used [35]. Data sources for each site are described in the methods.

site		bottom-up	SE	tower	upper bound uncertainty	lower bound uncertainty	'min{N : P}'
TAM-06	G_P^*	28.3	3.0	—			40.8
	R_C	6.3	2.5	—			9.5
	G_P	22.0	—	—			31.3
TAM-05	G_P^*	31.9	3.4	—			33.4
	R_C	7.5	3.0	—			6.4
	G_P	24.4	—	—			27.0
CAX-06	G_P^*	30.9	1.5	36.0			30.3
	R_C	6.4	0.1	—			5.4
	G_P	24.5	—	—			24.8
TAP-04	G_P^*	29.3	4.4	28.8	29.3	28.6	35.7
	R_C	7.4	4.0	—			7.9
	G_P	21.9		—			27.8
MAN-01	G_P^*	29.9	4.8	36.9	37.9	35.5	34.3
	R_C	10.0	4.0	—			6.6
	G_P	19.9	—	—			27.8
MAN-05	G_P^*	—	—	30.4			35.8
	R_C	—	—	—			7.4
	G_P	—	—	—			28.5
JARU	G_P^*	—	—	34.5	34.9	33.5	35.2
	R_C	—	—	—			7.1
	G_P	—	—	—			28.1

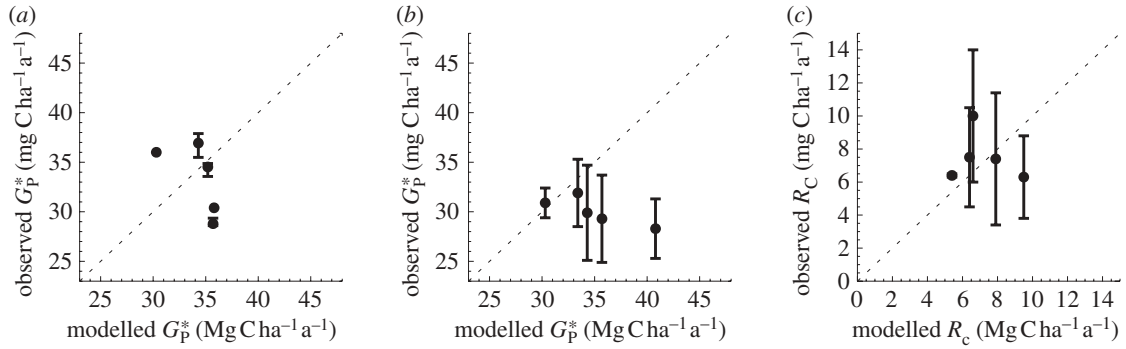

Figure 5. Model evaluation of simulated gross primary productivity (G_P^*), and leaf respiration (R_C) using available observations derived from (*a*) eddy correlation and (*b*,*c*) bottom-up. Error bars for eddy correlation measurements correspond to uncertainty [35] and correspond to standard error for bottom-up estimates. Data sources for each site are described in the methods.

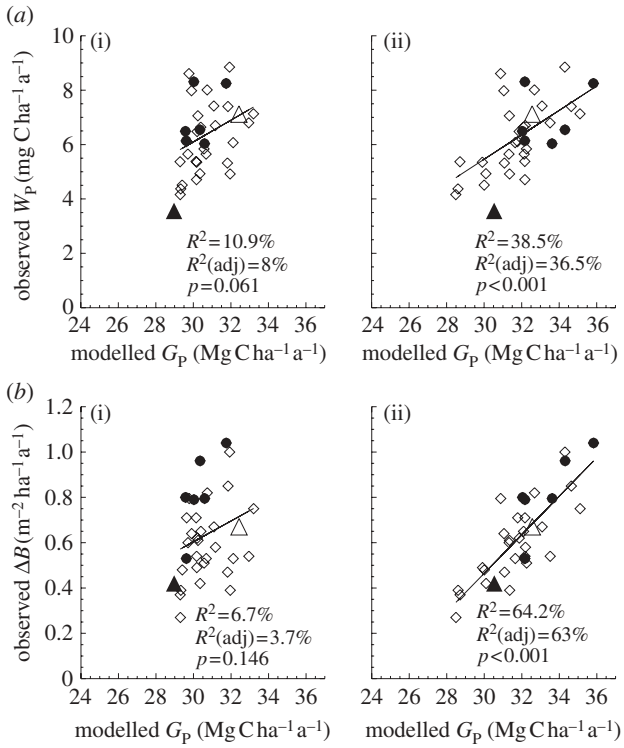

Figure 6. Relationships of simulated G_P against (*a*) observed stem growth (W_P) and (*b*) basal area growth (ΔB) [6] at 33 sites. Model configurations correspond to assumption of (i) N limitation (using $[N]_A$ only) and (ii) P limitation (using $[P]_A$ only) across all studied sites. Filled and open symbols correspond to N- and P-limited sites, respectively, according to equation (2.2). The triangle symbols correspond to sites with no available soil phosphorous data.

The modelling framework used in this study does not consider plant-related soil water stress. The stomatal conductance formulation used [41] takes into account drought stress via atmospheric vapour-pressure deficits. However, especially at forest sites with strong seasonality, there is a strong stomatal control of transpiration combined with deep rooting systems that allow water recharge from deep soils [59]. There is little evidence of soil water deficit effects on tropical forest productivity [32,59,60], except for the most peripheral forests close to the forest/savannah transition zone [9] and no such forests were considered in this study.

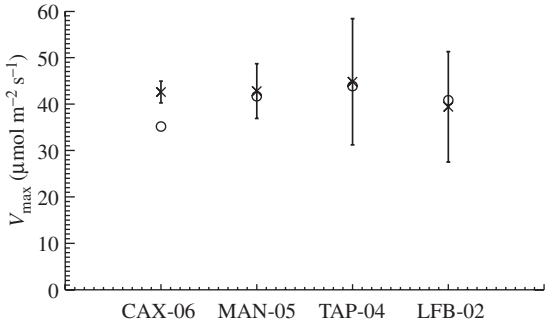

Figure 7. Comparison of top of the canopy V_{cmax} derived from gas exchange measurements at four rainforest sties in the Amazon Basin (crosses, error bars correspond to one standard deviation), and estimated in this study using the 'min{N : P}' relationship (circles). Data sources from Brazilian sites are Caxiuana from Vale *et al.* [46], Manaus from Carswell *et al.* [45] and Tapajos from Domingues *et al.* [47]. The Bolivian site LFB-02 is courtesy of T. F. Domingues, unpublished data.

(c) *Relating simulated net carbon uptake to measured stem wood production (W_P) and basal area growth (ΔB)*

In the analysis presented, we have shown that simulated G_P using 'min{N : P}' can explain approximately 30 per cent of observed variability in observed wood production including P-limitation alone or when including both N- and P-limitation. Including N-limitation with P-limitation marginally decreases the obtained correlation, and simulated G_P under N-limitation alone can only explain 15 per cent of the observed variability in W_P. However, from the seven N-limited sites (only six included in calculations of R^2), three presented N and P co-limitation. Additionally, our analysis suggests that variability in local meteorological variables given fixed nutrient levels at the various sites does not simulate variation in G_P sufficient to explain any of the observed variability of W_P and ΔB. Finally, using a species abundance weighting (equation (2.1)) to estimate leaf nutrients at each plot proved to have an impact on simulated G_p and its capability to explain variability of W_P and ΔB (adjusted R^2 of 26%, $p = 0.001$ and 60%, $p < 0.001$ respectively) as opposed to using plot level means which gave lower correlations and significance levels (adjusted R^2 of 15%, $p = 0.016$ and 23%, $p = 0.003$ respectively, not shown).

Our simulations gave only a limited variability in G_P for the 38 sites simulated (with 95% of G_P estimates within 10% of our overall basin-wide means). These small variations in simulated G_P explained up to 26 and 60 per cent of the observed variability in W_P and ΔB, respectively. This suggests not only that variations in W_P for the forests examined may indeed be driven to a considerable extent by variations in G_P (themselves driven by variations in canopy nutrient concentrations, and especially by variations in phosphorus), but also that as G_P increases beyond a certain point, then much of the extra carbohydrate availability is preferentially allocated towards W_P. For example, at a low G_P of 25 Mg C ha^{-1} a^{-1} as simulated by the 'min{N : P}' model, W_P is estimated at 3.9 Mg C ha^{-1} a^{-1} equal to just 0.16 of G_P. But at a higher G_P of 35 Mg C ha^{-1} a^{-1}, W_P is estimated at 11.3 Mg C ha^{-1} a^{-1}, equal to 0.32 of G_P. This is as suggested by Lloyd & Farquhar [61] and has important implications for any stimulation of G_P as might be expected to occur, for example, in response to elevated [CO_2] with any stimulation of W_P being proportionally much higher than any associated increase in G_P.

For ΔB, the differences are even more profound with the ratio $\Delta B/G_P$ varying more than threefold from 0.012 to 0.037 m^2 Mg^{-1}C for the same simulated G_P variations. This greater relative sensitivity is due to a consistent decline in tree-wood density with increasing G_P. Indeed, based on data presented by Baker *et al.* [38,62], we have also estimated changes in stand-level wood density ($\hat{\rho}_w$) and found even stronger relationships with G_P than for either W_P or ΔB with R^2 of 0.76 and a slope of around 40 mol μmol kg m^{-1} s^{-1} (results not shown). For example, $\hat{\rho}_w$ at a low G_P of 25 Mg C ha^{-1} a^{-1} as simulated by the 'min{N : P}' model is estimated at 730 kg m^{-3}, but it is also estimated that $\hat{\rho}_w$ would be only 331 kg m^{-3} for G_P of 35 Mg C ha^{-1} a^{-1}. Thus, higher productivity sites are also characterized by a greater abundance of species characterized by a low $\hat{\rho}_w$ capable of high rates of basal area (and presumably height) growth.

Variability in carbon use efficiency (CUE), the ratio of net primary productivity to G_P^*, across the studied transect owing to variability in autotrophic respiration rates has been proposed as a possible explanation for the observed spatial variability in observed rates of stem wood productivity [1]. This hypothesis suggests lower rates of CUE owing to higher plant respiration at low productivity sites and higher rates of CUE and lower plant respiration rates at the high productivity sites. Ongoing fieldwork campaigns at various sites across the Amazon Basin are currently measuring the individual carbon cycle components. This type of research should lead to a better understanding of (i) variability of main fluxes across the Amazon Basin and, most importantly, (ii) the mechanism behind a possible variability in plant respiration as proposed, and its relationship to nutrient supply, which as shown in the present analysis has a major role in influencing observed spatial variability in stem productivity across the Amazon Basin.

Global vegetation models, which ignore phosphorus availability [63,64], would not predict at least some of the observed spatial variability in stem growth-rates that clearly occurs across the Amazon Basin. This variability appears to be of fundamental ecological importance, because it is closely correlated in space with similar variation in carbon stores (biomass), stand-level species composition, wood density and population dynamics, and with underlying soil properties. The likelihood, therefore, is that these macroecological gradients will prove important in determining forest responses to global change drivers such as increasing [CO_2] and temperatures, as well as determining how forest ecosystems may respond to other more local drivers. For example, it has been suggested that western Amazon forests are less sensitive than eastern forests to some forms of anthropogenic disturbance, because they are adapted to the naturally much higher turnover rates of these forests compared with the eastern part of the Basin [65,66]. Clearly, global-scale models need to be able to reproduce the present-day spatial variation in tree growth-rates across the Amazon and to include any relevant additional process parametrizations, in our specific case effects of soil fertility on foliar [P] and hence on simulated net carbon uptake. Such advances should lead to an enhanced ability of global models to simulate the response of tropical ecosystems to future changes in climate and atmospheric composition, and to improved quantification of future climate–carbon cycle feedbacks.

5. SUMMARY

We have simulated the sensitivity of G_P to parametrizations of photosynthetic capacity, in order to understand spatial dynamics of observed W_P. We tested model sensitivity to including nutrient (N and P, only N, and only P) constraints on photosynthesis, and how the simulated photosynthesis relates to variables such as above-ground growth and biomass. In agreement with previous studies showing soil phosphorous as the principal soil fertility factor influencing rates of tree growth across the Amazon Basin, simulations performed in this study suggest that when including a leaf [P] constraint to photosynthetic capacity, simulated G_P agrees with the few available observations and can explain up to approximately 30 per cent of the spatial variability in stem growth. Incorporating this improved understanding of the role of soil nutrients in explaining basin-wide variations in G_P will lead to improved parametrizations in global carbon cycle models. This should enable improved simulation of the response of tropical ecosystems to future changes in climate and atmospheric composition, and improved quantification of future climate–carbon cycle feedbacks.

Sandra Patiño and Samuel Almeida, two of our co-authors, have left us during the process of the submission and publication of this paper. We would like to dedicate this piece of work to both of them. Financial support for L.M. was provided through the EU Project 'Carbonsink-LBA Proposal no. EVK 1999–0191' with most of the modelling work being done at the Max Planck Institute for Biogeochemistry, Jena, Germany. The final analysis was also supported through the UK NERC Tropical Biomes in Transition (TROBIT) consortium, UK Natural Environment Research Council (NERC) grant (NE/A/S/2003/00608/2) and the UK NERC Amazon Integrated Carbon Analysis—(AMAZONICA) consortium grant (NE/F005997/1). O.P. was partially funded through the European Union-funded PANAMAZONIA

programme. N.M.F. is supported by a Marie Curie Intra-European Fellowship within the 7th European Community Framework Programme. G.P.W. was supported by the Joint DECC/Defra Met Office Hadley Centre Climate Programme—(GA01101). We also thank Gabriela López-Gonzalez for developing the forest productivity and biomass database, with funding from the Gordon and Betty Moore Foundation (grant to RAINFOR) and the School of Geography, University of Leeds. The RAINFOR programme is supported by the Gordon and Betty Moore Foundation. RAINFOR field campaigns contributing to this study were funded by the Royal Geographical Society, CARBONSINK-LBA and the Max Planck Institute for Biogeochemistry, Jena, Germany. We gratefully acknowledge the support and funding of organizations who have contributed to the establishment and maintenance of individual sites: Natural Environment Research Council, EU Framework V and VI, US National Geographical Society, WWF-US/Garden Club of America, US National Science Foundation, the Nature Conservancy/Mellon Foundation (Ecosystem Function Programme), Conselho Nacional de Desenvolvimento Cientifico e Tecnológico, Museu Goeldi, Estacao Cientifica Ferreira Penna, Andrew W. Mellon Foundation, NASA-LBA Programme, Conservation, Food and Health Foundation, MacArthur Foundation, Fundación Jatun Sacha, Estación Científica Yasuní de la Pontificia Universidad Católica del Ecuador, Estación de Biodiversidad Tiputini, Conservation International, ACEER, Albergue Inkaterra, Explorama Tours S.A., Explorers Inn, IIAP, INRENA, UNAP and UNSAAC. We thank two anonymous reviewers for comments on the manuscript. This paper constitutes Publication No. A/582 of the Royal Society South East Asia Rainforest Research Programme.

APPENDIX A

In addition to the min{N : P} equation, we investigated the utility of the V_{max} versus leaf P (area basis) relationship: the '$[P]_A$ only' relationship as obtained in Mercado *et al.* [10] with the 'A' subscript here used to denote values expressed on a leaf area basis. This relationship was obtained by relating the best-fitted top of the canopy V_{max} from each of five calibration sites, against measured upper canopy $[N]_A$ and $[P]_A$ for the same sites. The relationship for $[N]_A$ ('$[N]_A$ only') was very poor ($R^2 = 0.08$), but much better for $[P]_A$ ($R^2 = 0.41$). $\mathcal{J}_{max}$ has been estimated as a constant ratio (r) of V_{max} as calibrated in the modelling exercise of Mercado *et al.* [10],

$$\left.\begin{aligned} V_{max} &= a[P]_A + b \\ \text{and} \quad \mathcal{J}_{max} &= rV_{max} \end{aligned}\right\}, \tag{A 1}$$

with corresponding values for a, b and r of 386.9 μmol $m^{-2}\,s^{-1}$, 17.9 μmol $g^{-1}\,s^{-1}$ and 1.92, respectively. Respective values for the slope, intercept and r for the '$[N]_A$ only' relationship are 6.8 μmol $m^{-2}\,s^{-1}$, 30.8 17.9 μmol $g^{-1}\,s^{-1}$ and 1.92.

REFERENCES

1 Malhi, Y. *et al.* 2004 The above-ground coarse wood productivity of 104 Neotropical forest plots. *Glob. Change Biol.* **10**, 563–591. (doi:10.1111/j.1529-8817.2003.00778.x)
2 Phillips, O. L. *et al.* 2004 Pattern and process in Amazon tree turnover, 1976–2001. *Phil. Trans. R. Soc. Lond. B* **359**, 381–407. (doi:10.1098/rstb.2003.1438)
3 Baker, T. R. *et al.* 2004 Variation in wood density determines spatial patterns in Amazonian forest biomass. *Glob. Change Biol.* **10**, 545–562. (doi:10.1111/j.1529-8817.2003.00751.x)
4 Quesada, C. A., Lloyd, J., Anderson, L. O., Fyllas, N. M., Schwarz, M. & Czimczik, C. I. 2009 Soils of Amazonia with particular reference to the rainforest sites. *Biogeosciences* **8**, 1415–1440. (doi:10.5194/bg-8-1415-2011)
5 Quesada, C. A. *et al.* 2010 Variations in chemical and physical properties of Amazon forest soils in relation to their genesis. *Biogeosciences* **7**, 1515–1541. (doi:10.5194/bg-7-1515-2010)
6 Quesada, C. A. *et al.* 2009 Regional and large-scale patterns in Amazon forest structure and function are mediated by variations in soil physical and chemical properties. *Biogeosci. Discuss.* **6**, 3993–4057. (doi:10.5194/bgd-6-3993-2009)
7 Fyllas, N. M. *et al.* 2009 Basin-wide variations in foliar properties of Amazonian forest: phylogeny, soils and climate. *Biogeosciences* **6**, 2677–2708. (doi:10.5194/bg-6-2677-2009)
8 Aragão, L. E. O. *et al.* 2009 Above- and below-ground net primary productivity across ten Amazonian forests on contrasting soils. *Biogeosciences* **6**, 2759–2778. (doi:10.5194/bg-6-2759-2009)
9 Lloyd, J., Goulden, M., Ometto, J. P., Fyllas, N. M., Quesada, C. A. & Patiño, S. 2009 Ecophysiology of forest and savanna vegetation. In *Amazonia and climate change* (eds M. Keller, J. Gash & P. D. Silva), pp. 463–484. Washington, DC: American Geophysical Union.
10 Mercado, L. M., Lloyd, J., Dolman, A. J., Sitch, S. & Patiño, S. 2009 Modelling basin-wide variations in Amazon forest productivity. 1. model calibration, evaluation and upscaling functions for canopy photosynthesis. *Biogeosciences* **6**, 1247–1272. (doi:10.5194/bg-6-1247-2009)
11 Evans, J. R. 1993 Photosynthetic acclimation and nitrogen partitioning within a lucerne canopy. I. Canopy characteristics. *Aust. J. Plant Physiol.* **20**, 55–67. (doi:10.1071/PP9930055)
12 Martinelli, L. A., Piccolo, M. C., Townsend, A. R., Vitousek, P. M., Cuevas, E., McDowell, W., Robertson, G. P., Santos, O. C. & Treseder, K. 1999 Nitrogen stable isotopic composition of leaves and soil: tropical versus temperate forests. *Biogeochemistry* **46**, 45–65. (doi:10.1023/A:1006100128782)
13 Ometto, J. *et al.* 2006 The stable carbon and nitrogen isotopic composition of vegetation in tropical forests of the Amazon Basin, Brazil. *Biogeochemistry* **79**, 251–274. (doi:10.1007/s10533-006-9008-8)
14 Nardoto, G. B., Ometto, J., Ehleringer, J. R., Higuchi, N., Bustamante, M. M. D. & Martinelli, L. A. 2008 Understanding the influences of spatial patterns on N availability within the Brazilian Amazon forest. *Ecosystems* **11**, 1234–1246. (doi:10.1007/s10021-008-9189-1)
15 Vitousek, P. M. 1984 Litterfal, nutrient cycling nutrient limitation in tropical forests. *Ecology* **65**, 285–298. (doi:10.2307/1939481)
16 Lloyd, J., Bird, M., Veenendaal, E. M. & Kruijt, B. 2001 Should phosphorus availability be constraining moist tropical forest responses to increasing CO_2 concentrations? In *Global biogeochemical cycles in the climate system* (eds E. D. Schulze, S. P. Harrison, M. Heimann, E. A. Holland, J. Lloyd & I. C. Prentice), pp. 96–114. San Diego, CA: Academic Press.
17 Reich, P. B., Oleksyn, J. & Wright, I. J. 2009 Leaf phosphorus influences the photosynthesis–nitrogen relation: a cross-biome analysis of 314 species. *Oecologia* **160**, 207–212. (doi:10.1007/s00442-009-1291-3)

18 Domingues, T. F. *et al.* 2010 Co-limitation of photosynthetic capacity by nitrogen and phosphorus in West Africa woodlands. *Plant Cell Environ.* **33**, 959–980. (doi:10.1111/j.1365-3040.2010.02119.x)

19 Farquhar, G. D. & von Caemmerer, S. 1982 Modelling of photosynthetic response to environmental conditions. In *Encyclopedia of plant physiology* (eds O. L. Lange, P. S. Nobel, C. B. Osmond & H. Ziegler), pp. 549–587. Berlin, Germany: Springer.

20 Patiño, S. *et al.* 2009 Branch xylem density variations across the Amazon Basin. *Biogeosciences* **6**, 545–568. (doi:10.5194/bg-6-545-2009)

21 Tiessen, H. & Moir, J. O. 1993 Total and organic carbon. In *Soil sampling and methods of analysis* (ed. M.R. Carter), pp. 187–199, 2nd edn. Boca Raton, FL: CRC Press.

22 Keeling, H. C. & Phillips, O. L. 2007 A calibration method for the crown illumination index for assessing forest light environments. *For. Ecol. Manage.* **242**, 431–437. (doi:10.1016/j.foreco.2007.01.060)

23 Meir, P., Grace, J. & Miranda, A. C. 2000 Photographic method to measure the vertical distribution of leaf area density in forests. *Agric. For. Meteorol.* **102**, 105–111. (doi:10.1016/S0168-1923(00)00122-2)

24 Keeling, R. F., Piper, S. C., Bollenbacher, A. F. & Walker, J. S. 2009 Atmospheric CO_2 records from sites in the SIO air sampling network. In *Trends: a compendium of data on global change.* Oak Ridge, TN: Carbon Dioxide Information Analysis Center, Oak Ridge National Laboratory, U.S. Department of Energy.

25 Lloyd, J. *et al.* 1996 Vegetation effects on the isotopic composition of atmospheric CO_2 at local and regional scales: theoretical aspects and a comparison between rain forest in Amazonia and a boreal forest in Siberia. *Aust. J. Plant Physiol.* **23**, 371–399. (doi:10.1071/PP9960371)

26 Weedon, G. P., Gomes, S., Viterbo, P., Oesterle, H., Adam, J. C., Bellouin, N., Boucher, O. & Best, M. 2010 The WATCH Forcing Data 1958–2001: a meterological forcing dataset for land surface- and hydrological-models. WATCH Technical report no 22, 41pp. (available at www.eu-watch.org/publications).

27 Weedon, G. P. *et al.* In press. Creation of the WATCH Forcing Data and its use to assess global and regional reference crop evaporation over land during the twentieth century. *J. Hydrometeol.* (doi:10.1175/2011JHM1369.1)

28 Lloyd, J. *et al.* 2010 Optimisation of photosynthetic carbon gain and within-canopy gradients of associated foliar traits for Amazon forest trees. *Biogeosciences* **7**, 1833–1859. (doi:10.5194/bg-7-1833-2010)

29 Metcalfe, D. B. *et al.* 2007 Factors controlling spatio-temporal variation in carbon dioxide efflux from surface litter, roots, and soil organic matter at four rain forest sites in the eastern Amazon. *J. Geophys. Res. Biogeosci.* **112**, G04001. (doi:10.1029/2007JG000443)

30 Metcalfe, D. B. *et al.* 2008 The effects of water availability on root growth and morphology in an Amazon rainforest. *Plant Soil.* **311**, 189–199. (doi:10.1007/s11104-008-9670-9)

31 Malhi, Y. *et al.* 2009 Comprehensive assessment of carbon productivity, allocation and storage in three Amazonian forests. *Glob. Change Biol.* **15**, 1255–1274. (doi:10.1111/j.1365-2486.2008.01780.x)

32 Goulden, M. L., Miller, S. D., da Rocha, H. R., Menton, M. C., de Freitas, H. C., Figueira, A. & de Sousa, C. 2004 Diel and seasonal patterns of tropical forest CO_2 exchange. *Ecol. Appl.* **14**, S42–S54. (doi:10.1890/02-6008)

33 Hutyra, L. R., Munger, J. W., Saleska, S. R., Gottlieb, E., Daube, B. C., Dunn, A. L., Amaral, D. F., de Camargo, P. B. & Wofsy, S. C. 2007 Seasonal controls on the exchange of carbon and water in an Amazonian rain forest. *J. Geophys. Res. Biogeosci.* **112**, G03008. (doi:10.1029/2006jg000365)

34 Saleska, S. R. *et al.* 2003 Carbon in Amazon forests: Unexpected seasonal fluxes and disturbance-induced losses. *Science* **302**, 1554–1557. (doi:10.1126/science.1091165)

35 Restrepo-Coupe, N. *et al.* In preparation. Gross ecosystem productivity seasonality in the tropics: issues posed by the absence of CO_2 profile measurements at eddy flux systems.

36 Saleska, S. R., da Rocha, H. R., Huete, A. R., Nobre, A. D., Artaxo, P. & Shimabukuro, Y. E. 2009 *LBA-ECO CD-32 Brazil Flux Network Integrated Data:1999–2006*. Sao Paulo, Brazil: National Institute for Space Research (INPE/CPTEC), Cachoeira Paulista. See (http://www.daac.ornl.gov) from Oak Ridge National Laboratory Distributed Active Archive Center, Oak Ridge, Tennessee, U.S.A. and (http://lba.cptec.inpe.br/) from LBA Data and Information System.

37 Peacock, J., Baker, T. R., Lewis, S. L., Lopez-Gonzalez, G. & Phillips, O. L. 2007 The RAINFOR database: monitoring forest biomass and dynamics. *J. Veg. Sci.* **18**, 535–542. (doi:10.1111/j.1654-1103.2007.tb02568.x)

38 Baker, T. R. *et al.* 2004 Increasing biomass in Amazonian forest plots. *Phil. Trans. R. Soc. Lond. B* **359**, 353–365. (doi:10.1098/rstb.2003.1422)

39 Mercado, L., Lloyd, J., Carswell, F., Malhi, Y., Meir, P. & Nobre, A. D. 2006 Modelling Amazonian forest eddy covariance data: a comparison of big leaf versus sun/shade models for the C-14 tower at Manaus I. Canopy photosynthesis. *Acta Amazonica* **36**, 69–82. (doi:10.1590/S0044-59672006000100009)

40 de Pury, D. G. G. & Farquhar, G. D. 1997 Simple scaling of photosynthesis from leaves to canopies without the errors of big-leaf models. *Plant Cell Environ.* **20**, 537–557. (doi:10.1111/j.1365-3040.1997.00094.x)

41 Cowan, I. R. & Farquhar, G. D. 1977 Stomatal function in relation to leaf metabolism and environment. In *Integration of activity in the higher plant* (ed. D. H. Jennings), pp. 471–505. Cambridge, UK: Cambridge University Press.

42 Atkin, O. K., Evans, J. R., Ball, M. C., Lambers, H. & Pons, T. L. 2000 Leaf respiration of snow gum in the light and dark. Interactions between temperature and irradiance. *Plant Physiol.* **122**, 915–923. (doi:10.1104/pp.122.3.915)

43 Gusewell, S. 2004 N : P ratios in terrestrial plants: variation and functional significance. *New Phytol.* **164**, 243–266. (doi:10.1111/j.1469-8137.2004.01192.x)

44 Aerts, R. & Chapin, F. S. 2000 The mineral nutrition of wild plants revisited: a re-evaluation of processes and patterns. *Adv. Ecol. Res.* **30**, 1–67. (doi:10.1016/S0065-2504(08)60016-1)

45 Carswell, F. E., Meir, P., Wandelli, E. V., Bonates, L. C. M., Kruijt, B., Barbosa, E. M., Nobre, A. D., Grace1, J. & Jarvis, P. G. 2000 Photosynthetic capacity in a central Amazonian rain forest. *Tree Physiol.* **20**, 179–186. (doi:10.1093/treephys/20.3.179)

46 Vale, R. L., Maroco, J. P., Carvalho, C. R. J., Almeida, S., Meir, P., Grace, J., Pereira, J. S. & Chaves, M. M. 2003 Carbon assimilation in an Amazonian rainforest: a rain exclusion experiment. In *Abstracts of the Annual Main Meeting of the Society for Experimental Biology, Southampton, UK, 31 March–4 April, 2003. Comp. Biochem. Physiol. A* **134**, S186.

47 Domingues, T. F., Martinelli, L. A. & Ehleringer, J. R. 2007 Ecophysiological traits of plant functional groups

in forest and pasture ecosystems from eastern Amazonia, Brazil. *Plant Ecol.* **193**, 101–112. (doi:10.1007/s11258-006-9251-z)

48 Coste, S., Roggy, J. C., Imbert, P., Born, C., Bonal, D. & Dreyer, E. 2005 Leaf photosynthetic traits of 14 tropical rain forest species in relation to leaf nitrogen concentration and shade tolerance. *Tree Physiol.* **25**, 1127–1137. (doi:10.1093/treephys/25.9.1127)

49 Meir, P., Levy, P. E., Grace, J. & Jarvis, P. G. 2007 Photosynthetic parameters from two contrasting woody vegetation types in West Africa. *Plant Ecol.* **192**, 277–287. (doi:10.1007/s11258-007-9320-y)

50 Clark, D. A., Brown, S., Kicklighter, D. W., Chambers, J. Q., Thomlinson, J. R., Ni, J. & Holland, E. A. 2001 Net primary production in tropical forests: an evaluation and synthesis of existing field data. *Ecol. Appl.* **11**, 371–384. (doi:10.1890/1051-0761(2001)011[0371:NPPITF]2.0.CO;2)

51 Hutyra, L. R., Munger, J. W., Hammond-Pyle, E., Saleska, S. R., Restrepo-Coupe, N., Daube, B. C., de Camargo, P. B. & Wofsy, S. C. 2008 Resolving systematic errors in estimates of net ecosystem exchange of CO_2 and ecosystem respiration in a tropical forest biome. *Agric. For. Meteorol.* **148**, 1266–1279. (doi:10.1016/j.agrformet.2008.03.007)

52 Aubinet, M., Heinesch, B. & Longdoz, B. 2002 Estimation of the carbon sequestration by a heterogeneous forest: night flux corrections, heterogeneity of the site and inter-annual variability. *Glob. Change Biol.* **8**, 1053–1071. (doi:10.1046/j.1365-2486.2002.00529.x)

53 Massman, W. J. & Lee, X. 2002 Eddy covariance flux corrections and uncertainties in long-term studies of carbon and energy exchanges. *Agric. For. Meteorol.* **113**, 121–144. (doi:10.1016/S0168-1923(02)00105-3)

54 Pattey, E., Strachan, I. B., Desjardins, R. L. & Massheder, J. 2002 Measuring nighttime CO_2 flux over terrestrial ecosystems using eddy covariance and nocturnal boundary layer methods. *Agric. For. Meteorol.* **113**, 145–158. (doi:10.1016/S0168-1923(02)00106-5)

55 Kruijt, B. *et al.* 2004 The robustness of eddy correlation fluxes for Amazon rain forest conditions. *Ecol. Appl.* **14**, S101–S113. (doi:10.1890/02-6004)

56 Luyssaert, S. *et al.* 2007 CO_2 balance of boreal, temperate, and tropical forests derived from a global database. *Glob. Change Biol.* **13**, 2509–2537. (doi:10.1111/j.1365-2486.2007.01439.x)

57 Reich, P. B., Tjoelker, M. G., Pregitzer, K. S., Wright, I. J., Oleksyn, J. & Machado, J. L. 2008 Scaling of respiration to nitrogen in leaves, stems and roots of higher land plants. *Ecol. Lett.* **11**, 793–801. (doi:10.1111/j.1461-0248.2008.01185.x)

58 Meir, P., Grace, J. & Miranda, A. C. 2001 Leaf respiration in two tropical rainforests: constraints on physiology by phosphorus, nitrogen and temperature. *Funct. Ecol.* **15**, 378–387.

59 von Randow, C. *et al.* 2004 Comparative measurements and seasonal variations in energy and carbon exchange over forest and pasture in South West Amazonia. *Theor. Appl. Climatol.* **78**, 5–26. (doi:10.1007/s00704-004-0041-z)

60 Nepstad, D. C. *et al.* 1994 The role of deep roots in the hydrological and carbon cycles of Amazonian forest and pastures. *Nature* **372**, 666–669. (doi:10.1038/372666a0)

61 Lloyd, J. & Farquhar, G. D. 1996 The CO_2 dependence of photosynthesis, plant growth responses to elevated atmospheric CO_2 concentrations and their interaction with soil nutrient status.1. General principles and forest ecosystems. *Funct. Ecol.* **10**, 4–32.

62 Baker, T. R. *et al.* 2009 Do species traits determine patterns of wood production in Amazonian forests? *Biogeosciences* **6**, 297–307. (doi:10.5194/bg-6-545-2009)

63 Sitch, S. *et al.* 2003 Evaluation of ecosystem dynamics, plant geography and terrestrial carbon cycling in the LPJ dynamic global vegetation model. *Glob. Change Biol.* **9**, 161–185. (doi:10.1046/j.1365-2486.2003.00569.x)

64 Clark, D. B. *et al.* 2011 The Joint UK Land Environment Simulator (JULES), model description, part 2: carbon fluxes and vegetation. *Geosci. Model Dev. Discuss.* **4**, 641–688. (doi:10.5194/gmdd-4-641-2011)

65 Phillips, O. L., Rose, S., Mendoza, A. M. & Vargas, P. N. 2006 Resilience of southwestern Amazon forests to anthropogenic edge effects. *Conserv. Biol.* **20**, 1698–1710. (doi:10.1111/j.1523-1739.2006-00523.x)

66 Phillips, O. L. 2007 Drought, dispersal, and distribution in the inner tropics. *J. Biogeogr.* **34**, 1846–1847. (doi:10.1111/j.1365-2699.2007.01805.x)